Photochemical Formation and Reaction of Radical Pairs from NH_3−F_2 Complexes Isolated in Solid Argon[†]

Alexander V. Akimov,[‡] Ilia U. Goldschleger,[‡] Eugenii Ya. Misochko,[‡] and Charles A. Wight*[,§]

Institute of Problems of Chemical Physics of the Russian Academy of Sciences, 142432 Chernogolovka, Moscow Region, Russia, and Department of Chemistry, University of Utah, Salt Lake City, Utah 84112

Received: January 8, 2002; In Final Form: June 6, 2002

Photoinduced reactions in binary NH_3−F_2 complexes in solid argon are studied by FTIR spectroscopy. Analysis of the IR spectra and kinetics of product formation shows that the main photochemical channel at 355 nm is the formation of [$H_2N^\bullet$−HF···$F^\bullet$] radical pairs; the relative initial yield of this product is 0.55. We believe that this is the first observation of this mechanism of radical pair formation (i.e., by escape of one of the F atoms from the initial cage containing the complex). The other major product channels form FH_2N−HF and NH−HF−HF complexes in approximately equal amounts. Isotopic substitution experiments using $^{15}NH_3$ and ND_3 aided the assignments of the infrared bands of NH−HF−HF, which is identified for the first time. Thermal recombination of the [$H_2N^\bullet$−HF···$F^\bullet$] radical pairs at 20 K yields only the addition product FH_2N−HF. However, photoinduced recombination of [$H_2N^\bullet$−HF···$F^\bullet$] radical pairs at 633, 532, 355, and 266 nm gives predominantly NH−HF−HF complexes. The relative yield of this secondary photolysis product increases with increasing energy of photoexcitation and is close to unity at $\lambda \leq 355$ nm.

1. Introduction

Chemical reaction of fluorine atoms in cryogenic matrixes is an effective strategy for the formation and spectroscopic characterization of reactive intermediates; see, for example, the review by Jacox.[1] Recently, we have published several papers devoted to the study of reactions of mobile F atoms with molecules isolated in solid argon. Our primary interest has been the stabilization of open-shell products in reactions of the general type[2,3]

$$F + M \rightarrow FM^\bullet \quad (1a)$$

$$F + RH \rightarrow R^\bullet{-}HF \quad (1b)$$

This type of reaction is made possible by the high mobility of F atoms in argon after generation by photodissociation of F_2 isolated in the matrix. Kunntu et al. observed that, when F_2 is dissociated with light at $\lambda < 360$ nm, the two F atoms are practically unhindered by the normal cage effect.[4] The atoms fly apart and are stabilized in the matrix at a distance of ~3−5 lattice periods. Migration of the "hot" atoms and thermal diffusion of F atoms at $T > 20$ K allows F atoms to react with isolated molecules and enables the observation of reactions of types 1a and 1b.[5,6]

In contrast to photolysis of isolated F_2, photolysis of F_2 in binary M−F_2 complexes leads to closed-shell products in which all of the atoms are retained in the reaction cage

$$M{-}F_2 \xrightarrow{h\nu} MF_2 \quad (2a)$$

$$RH{-}F_2 \xrightarrow{h\nu} RF{-}HF \quad (2b)$$

Photochemical reactions of types 2a and 2b were studied earlier by infrared spectroscopy.[5,7−11] These reactions appeared to proceed directly, and no intermediates were observed. The possibility always exists for one of the F atoms to escape the reactant cage; in this case, we might expect the formation of a pair of stabilized radicals such as [$FM^\bullet$···$F^\bullet$] or [HF−$R^\bullet$···$F^\bullet$]. However, until now, this type of radical pair formation has not been observed. The subsequent recombination of these radical pairs could be stimulated by thermal annealing of the matrix or by photoexcitation of one of the radicals in the pair. We can thus investigate the possibility of stimulating recombination reactions of radical pairs in the ground and excited electronic states. In this study, we have attempted to realize such reactions in stabilized radical pairs [$H_2N^\bullet$−HF···$F^\bullet$], which form upon photolysis of NH_3−F_2 complexes in solid argon.

2. Experimental Details

The experimental techniques are similar to those used in our previous study.[3,5] Dilute mixtures of Ar/F_2 and Ar/NH_3 were deposited through separate stainless steel vacuum manifolds onto the surface of a CsI window held at 15 K in a high-vacuum chamber. A portion of the stainless steel deposition line for F_2/Ar gas mixtures (between the gas metering valve and the cold window) was immersed in liquid nitrogen during sample deposition to remove impurities formed by reactions in the manifold. The composition of typical samples was Ar/F_2/NH_3 = 1000/1/1, and in all of the experiments, the mole fraction of reactants (F_2 and NH_3) was 3×10^{-3} or less. The gases $^{14}NH_3$, Ar (Spectra Gases, 99.999%), $^{15}NH_3$, $^{14}ND_3$ (Spectra Gases, 99.0%), and F_2 (Spectra Gases, 10% in Ar) were used without further purification. The sample preparation manifold was passivated by allowing a few Torr of reagent (fluorine or ammonia) to rest in the line prior to sample preparation.

Fluorine atoms were generated by F_2 photolysis at 355 nm with the third harmonic of a Nd:YAG laser (Continuum model Surelite operating at 10 Hz).

[†] Part of the special issue "Jack Beauchamp Festschrift".

* To whom correspondence should be addressed. E-mail: Chuck.Wight@utah.edu.

[‡] Russian Academy of Sciences.

[§] University of Utah.

10.1021/jp0255076 CCC: $22.00
Published on Web 09/04/2002

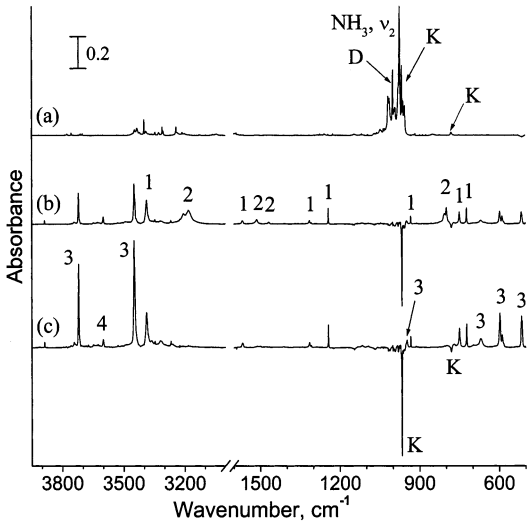

Figure 1. Infrared spectrum of Ar/F_2/$^{14}NH_3$ after deposition. Difference IR spectra (a) before and after (b) 2 and (c) 24 min of 355-nm photolysis at 5 mW/cm^2. The labeled bands correspond to NH_3−F_2 reactant complexes (K), ammonia dimers (D)H_2FN−HF complexes (**1**), [$H_2N^•$−HF···$F^•$] radical pairs (**2**), and NH−HF−HF complexes (**3**).

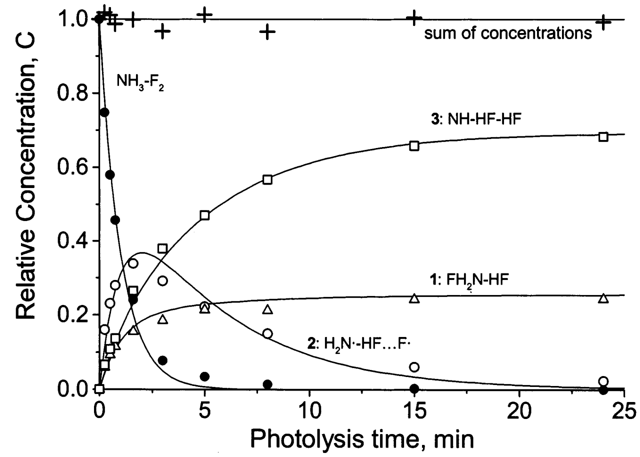

Figure 2. Photokinetics of products **1** (△), **2** (○), and **3** (□) and consumption of reactant NH_3−F_2 complexes (●) during 355-nm photolysis at 5 mW/cm^2. All concentrations are normalized to the initial concentration of NH_3−F_2. The sum of the concentrations of the reactant and products, $C_0 + C_1 + C_2 + C_3 + C_4$, is indicated by +. Solid curves correspond to the kinetics calculated using scheme 7 with parameters $k_1 = 1.00$ min^{-1}, $k_2 = 0.20$ min^{-1}, $\Phi_1 = 0.2$, $\Phi_2 = 0.55$, $\Phi_3 = 0.2$, $\Phi_4 = 0.05$, $\Phi'_1 = 0.1$, and $\Phi'_3 = 0.9$.

3. Results and Analysis

a. Photolysis of NH_3−F_2 Complexes at 15 K. Two representative regions of the infrared spectrum of a freshly prepared sample with Ar/F_2/NH_3 = 1000/1/1 are shown in Figure 1a. The spectrum exhibits several well-resolved bands that can be assigned to the NH_3 molecule.[12] The band at 1000 cm^{-1}, labeled D, is due to dimers of NH_3. The broad band at 966 cm^{-1}, labeled K in Figure 1a, was assigned earlier by Andrews and Lascola[10] to the reactant NH_3−F_2 complex. These authors ascribed the weak absorption at 781 cm^{-1} (labeled K in Figure 1a) to the perturbed F_2 vibrational mode in this complex. Our earlier experimental evidence supports their assignment of these bands.[3]

Laser photolysis at 355 nm leads to rapid disappearance of the reactant complex bands at 966 and 781 cm^{-1} (see Figure 1b). This occurs with a characteristic time constant of about 1 min when the average photolysis power is 5 mW/cm^{-2}, and the bands disappear completely after 10 min, as shown in Figure 2. Spectra obtained during and after photolysis exhibit the corresponding growth of four separate series of product bands, which can be distinguished by their kinetic behavior.

The product bands labeled **1** in Figures 1 and 2 and Table 1 were assigned earlier by Andrews and Lascola[10] to the molecular complex FH_2N−HF. Figure 2 shows that this closed-shell complex is a primary photoproduct but it also exhibits very slow growth in the later stages of photolysis, after all of the reactant complexes have been destroyed. The broad doublet bands at 799/806 and 3180/3206 cm^{-1} labeled **2** exhibit rapid growth in the initial stage of photolysis and slower diminution in the later stages, characteristic of a photochemical intermediate species. Strong bands observed at 3721 and 3450 cm^{-1} (labeled **3**) grow initially at a rate similar to that of **1**, but they continue to grow slowly during the later stages of photolysis when **1** is nearly constant and **2** is diminishing slowly. The growth of a single band **4** at 3626 cm^{-1} (not shown in Figure 2) correlates with the kinetics of reactant consumption.

In our previous paper,[3] we showed that 355-nm photolysis of NH_3−F_2 reactant complexes in argon occurs with a photochemical rate constant that is 10−20 times faster than the photodissociation of isolated F_2. Because the photolysis periods used in these experiments are too short to allow significant dissociation of isolated F_2 molecules, the observed products can be assigned exclusively to reactions of NH_3−F_2 complexes. We have determined the relative yields of the different product channels, C_i, based on a mass balance assuming that the sum of the product concentrations is equal to the consumption of the reactant complexes, ΔC_0

$$\Delta C_0 = C_1 + C_2 + C_3 + C_4 \quad (3)$$

Following the detailed procedure described previously,[6] this analysis involves determination of the relative infrared absorption cross sections of the reaction products from four different spectra in which the relative concentrations of products are different.

Figure 2 shows the changes in product concentrations normalized to the initial reactant concentration. An indication

TABLE 1: Infrared Bands and Their Assignments to Photolysis Products of Ar/F_2/$^{14}NH_3$ = 1000:1:1 Sample at 15 K

product **1** (FH_2N−HF)	product **2** ([$H_2N^•$−HF···$F^•$])	product **3** (NH−HF−HF)	complex[a] $H_2N^•$−HF	complex[b] FH_2N−HF
		513/515 (s)		
		597 (s)		
		699 (m, brd)		
722 (s)				723, ν_1
750 (s)				750, ν_1
	799/806 (s)		791/797 (s), ν_5/ν_6	
933 (w)				934, ν_4
		947 (w, brd)		
1243 (s)				1244, ν_3
1314 (vw)				1314, $2\nu_1$
	1468 (vw)		1465 (w), $2\nu_5$ or $2\nu_6$	
	1514 (w)		1512 (w), ν_4	
1568				1568, ν_2
	3180/3206 (vs)		3267 (vs), ν_1	
3268 (vw)				3269, ν_1
3387 (vs)				3389, ν_s
		3450 (vs)		
		3721 (vs)		

[a] Values from ref 3. [b] Values from ref 10.

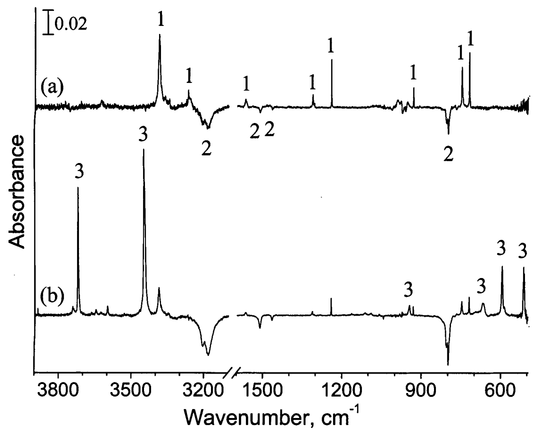

Figure 3. Difference IR spectra of samples prepared by 355-nm irradiation (to produce the maximum concentration of radical pairs **2**) before and after annealing at 20 K (trace a) and before and after 532-nm photolysis (25 min at 5 mW/cm^2) (trace b).

of the accuracy of the values is given by the sum of the relative concentrations (indicated by + in Figure 2), which deviates less than 5% from the ideal value of unity throughout the reaction. The main product of the sequence of photochemical reactions corresponds to band series **3**, $C_3 = 0.70$. The final relative concentration of product **1** is $C_1 = 0.25$, and the final concentration of product **4** is estimated to be $C_4 = 0.05$. The concentration of the intermediate **2** reaches a maximum value of $C_2 = 0.35$ during the initial stages of photolysis, and practically disappears during the following 15 min of photolysis at 5 mW/cm^2.

If photolysis is interrupted at the point where the concentration of intermediate **2** is a maximum (~2 min of photolysis) and the sample is subsequently annealed for 1−3 min at 19−20 K, the bands of series **2** disappear almost completely. Simultaneously, the bands of series **1** appear in their place. No other changes in the spectra take place under these conditions. Figure 3a shows this thermally activated conversion of intermediate **2** into product **1**.

b. Reactions of Diffusing F Atoms with NH_3 and NH_2−HF at 20 K. In the earlier work of Andrews and Lascola,[10] the bands of product **1** were assigned to the molecular complex FH_2N−HF, on the basis of a comparison with the calculated frequencies of FH_2N and the observed $^{15}N/^{14}N$ and H/D isotopic shifts. The bands of intermediate **2** were not reported in the earlier work. Table 1 shows that the bands of series **2** are very similar to infrared bands that were previously identified as arising from the radical molecule complex $H_2N^•$−HF, reported in our previous paper,[3] on the basis of FTIR and EPR spectroscopy. These complexes were formed by reaction of thermally diffusing F atoms with isolated NH_3 molecules during annealing of photolyzed samples at $T > 19$ K

$$F + NH_3 \rightarrow H_2N^• - HF \qquad (4)$$

In reaction 4, the complex $H_2N^•$−HF is stabilized in argon lattice sites previously occupied by NH_3 molecules. The same complex is formed upon photolysis of NH_3−F_2 complexes if the partner F atom is stabilized outside the initial reactant cage

$$NH_3 - F_2 \xrightarrow{h\nu} [H_2N^• - HF \cdots F^•] \qquad (5)$$

Such radical pairs $[H_2N^•-HF\cdots F^•]$ should recombine at temperatures where F atoms are mobile. The estimated diffusion constant of F atoms at 20 K is $D \approx 3 \times 10^{-15}$ cm^2 s^{-1}, and the time constant for each jump in the random walk through the lattice is $\tau \approx r_0^2/3D \approx 1$ s ($r_0 \approx 5 \times 10^{-8}$ cm).[11] This is sufficient time for thermal recombination to occur

$$[H_2N^• - HF \cdots F^•] \rightarrow FH_2N - HF \qquad (6)$$

To be certain that reaction 6 occurs, we made a series of experiments utilizing diffusing F atoms formed by photolysis of isolated F_2 molecules. The analogous experiments were performed earlier in mixtures with Ar/NH_3/F_2 = 1000/1/1.[3] In this study, we used mixtures with a higher F_2 concentration, namely, Ar/NH_3/F_2 = 1000/1/3, to distinguish between the primary reaction 4 and secondary reaction 6 of the diffusing F atoms with isolated NH_3. Reactions of diffusing atoms were studied by annealing of photolyzed samples at 20 K. Growth of the bands of the radical molecule complex $H_2N^•$−HF occurs at the beginning of the annealing period. As noted above, these bands are similar to those of band series **2** (see Table 1). Upon extended annealing, bands of another product begin to appear. These bands correspond to reaction product **1** and grow with a quadratic dependence compared to growth of the $H_2N^•$−HF complex bands. Such behavior demonstrates that in this experiment, product **1** is formed in secondary reactions of diffusing F atoms with the $H_2N^•$−HF complex. Additionally, it confirms the assignments of band series **2** to the complex $H_2N^•$−HF and of band series **1** to the complex FH_2N−HF.

It should be noted that the strong bands of product **2** at 799/806 and 3180/3206 cm^{-1} shown in Figure 1 are significantly broader than the corresponding bands of the $H_2N^•$−HF complex formed by the reaction of diffusing F atoms (eq 4). Also, the bands of the complex shown in Figure 1 at 3180/3206 cm^{-1} are shifted by 60−90 cm^{-1} relative to the HF bands of the isolated complex (see Table 1). These results demonstrate that the intermediate $H_2N^•$−HF formed in photoinduced reaction 5 has a distinct matrix environment compared with the complex formed by reaction of diffusing F atoms (eq 4). The observed perturbations are likely connected with the fact that the initial reactant complex has a distinct matrix environment (i.e., larger initial cage size) and with the presence of a second F atom stabilized nearby in the matrix.

c. Photolysis of $H_2N^•$−HF Complexes at 15 K. To determine the relative yield of products **1**−**3** from photolysis of the reactant complexes, we made some measurements of the band intensities at the beginning stages of the reaction when product growth is approximately linearly proportional to the photolysis period. For these measurements, we utilized a much lower laser photolysis light intensity (1 mW/cm^2). The resulting normalized initial yields of products **1**−**4** were $\Phi_1 = 0.20$, $\Phi_2 = 0.55$, $\Phi_3 = 0.20$, and $\Phi_4 = 0.05$.

The kinetic curves shown in Figure 2 demonstrate that the final distribution of products is determined by photolysis of the intermediate species **2**. To determine the relative product yields from photolysis of intermediate **2**, we photolyzed samples using four different wavelengths of laser light (633, 532, 355, and 266 nm). In these experiments, the initial 355-nm photolysis period was sufficient to consume the reactant complexes completely, and the concentration of complex **2** was past its maximum (approximately 7 min as shown in Figure 2). Subsequently, we photolyzed intermediate **2** until it was completely consumed. We observed that **2** is photolyzed even by 633-nm red light from a He−Ne laser, resulting in the formation of final products **1** and **3**. The relative yields of the two products are given in Table 2 for the four different wavelengths used. A representative spectrum showing the changes induced by the secondary photolysis at 532 nm is

TABLE 2: Wavelength-Dependent Quantum Yields of Products 1 and 3 Formed by Photolysis of [$H_2N^\bullet-HF\cdots F^\bullet$] Radical Pairs

wavelength (nm)	Φ'_1	Φ'_3
633	0.38	0.62
532	0.20	0.80
355	0.07	0.93
266	0.02	0.98

presented in Figure 3b. Upon photolysis at any of these wavelengths, the bands of product **3** are much stronger than those of **1**. At 633 nm, the relative yield of product **3** is $\Phi'_3 = 0.60$, which increases monotonically to $\Phi'_3 = 0.98$ at 266 nm. It should be noted that this distribution of products is very different from that of the thermal recombination reaction, which forms only product **1**, as shown in Figure 3a.

d. Kinetic Analysis and Assignment of the Infrared Bands. The observed data show that the photolysis of reactant complexes gives predominantly intermediate **2** and the subsequent photolysis of this intermediate determines the final distribution of products **1**, **3**, and **4**. Such a photochemical process can be described by a simple kinetic scheme that includes photolysis of reactants and intermediate **2**. The kinetic rates are

$$\begin{aligned} dC_0/dt &= -k_1C_0 \\ dC_1/dt &= k_1\Phi_1C_0 + k_2\Phi'_1C_2 \\ dC_2/dt &= k_1\Phi_2C_0 - k_2C_2 \\ dC_3/dt &= k_1\Phi_3C_0 + k_2\Phi'_3C_2 \\ dC_4/dt &= k_1\Phi_4C_0 \end{aligned} \tag{7}$$

The initial conditions are $C_0(0) = 1$, $C_1(0) = C_2(0) = C_3(0) = C_4(0) = 0$. The photochemical yields are normalized such that $\Phi_1 + \Phi_2 + \Phi_3 + \Phi_4 = 1$, $\Phi'_1 + \Phi'_3 = 1$, and the photochemical rate constants are given by $k_1 = 1/\tau_1$, $k_2 = 1/\tau_2$. Kinetic scheme 7 has a straightforward analytic solution, and the kinetic curves shown in Figure 2 were calculated using the rate constants k_i and yields Φ_i determined in separate experiments (vide supra). The analytic solution gives the final product distributions as $C_1 = \Phi_1 + \Phi_2\Phi_1$ and $C_3 = \Phi_3 + \Phi_2\Phi_3$, which are in good agreement with the experimental observations (as shown in Figure 2).

Band series **3** was observed earlier by Andrews and Lascola.[10] The two strong bands at 3450 and 3721 cm^{-1} were attributed to two conformational isomers of the molecular complex FH_2N-HF. However, an alternative assignment is to one complex containing two HF molecules (e.g, NH−HF−HF). We have observed that, under various experimental conditions (e.g., different photolysis wavelengths), the two bands always have the same intensity ratio. Andrews and Lascola noted some changes in the intensity ratio, and therefore made the assignment to two different species. However, we have not observed such changes. Additional evidence that product **3** does not contain the NH_2F moiety comes from the our failure to observe any bands in the region 1200−1600 cm^{-1}, which would correspond to the ν_2 and ν_3 bending modes in NH_2F. To provide a definite assignment of infrared bands at 3450 and 3721 cm^{-1}, a series of isotopic substitution experiments with $^{15}NH_3$ and $^{14}ND_3$ was performed. Figure 4 shows IR spectra of the products in samples $Ar/F_2/^{14}NH_3$, $Ar/F_2/^{15}NH_3$, and $Ar/F_2/^{14}ND_3$ in the spectral region of selected bands. The two bands exhibit no shift with ^{15}N substitution, but have large shifts in the deuterated samples. Therefore, both bands have to be ascribed to HF molecular vibrations, and all of the bands of series **3** have to be assigned to a molecular complex containing two HF molecules, NH−HF−HF. Infrared bands of NH−HF−HF generated by photolysis of $Ar/F_2/^{14}NH_3$, $Ar/F_2/^{15}NH_3$, and $Ar/F_2/^{14}ND_3$ samples are listed in Table 3.

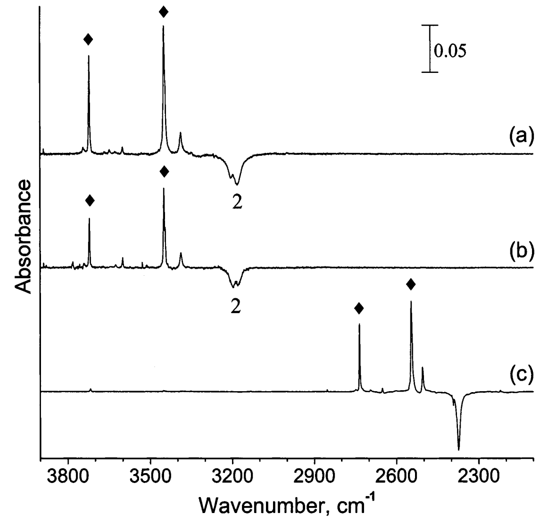

Figure 4. Difference IR bands of product **3** (labeled ♦) formed by photoinduced recombination of radical pairs in samples containing (a) $Ar/F_2/^{14}NH_3$, (b) $Ar/F_2/^{15}NH_3$, and (c) $Ar/F_2/^{14}ND_3$. Experimental conditions correspond to those of Figure 3b.

TABLE 3: Infrared Bands of Isotopomers of Product 3

^{14}NH−HF−HF	^{15}NH−HF−HF	^{14}ND−DF−DF
512.0/514.0 (s)	513.0/515.0	504.0
597.0 (s)	597.0	
669.0 (m, brd)	669	719.0
947.5 (w)	947.5	
3449.5 (vs)	3449.5	2546.0
3721.0 (vs)	3721.5	2734.0

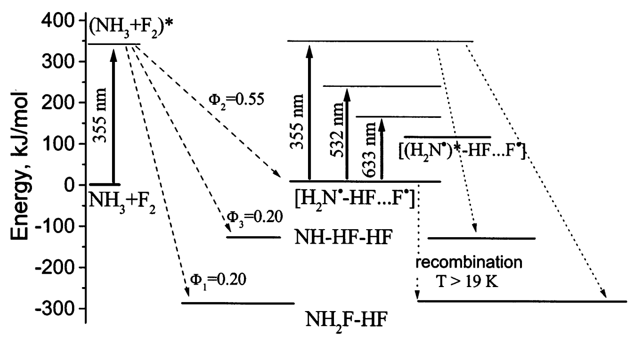

Figure 5. Energy diagram of photoinduced reactions of NH_3-F_2 complexes.

The yield of NH−HF−HF that is formed directly from reactant complexes is relatively low, about 20% according to our kinetic analysis. Also, the yield of this product is negligible in the thermal recombination reaction of [$H_2N^\bullet-HF\cdots F^\bullet$]. However, NH−HF−HF is the main product formed from photolysis of [$H_2N^\bullet-HF\cdots F^\bullet$] radical pairs, as shown in Table 2.

Unfortunately, we were unable to make a definitive identification of the minor product **4**, which accounts for 5% of the overall product yield.

Bearing in mind these spectroscopic assignments, an energy diagram of the major species involved was prepared as illustrated in Figure 5. Energies of the reactant and product species NH_3, NH_2, NH, and HF were taken from known enthalpies of formation.[14] Energies of NH_2F and the NH_2-HF complex were determined by the use of ab initio calculations using the Gaussian 98 program package [B3LYP/6-311++G(3df,2p)].[15]

The main channel of photodissociation of reactant complexes is formation of radical pairs, reaction 5. Alternatively, both hot F atoms can react with NH_3 in the reactant cage, forming the products FH_2N-HF and NH−HF−HF with approximately equal yields. This situation is to be contrasted with the case in which two thermally diffusing F atoms react with NH_3 to form only the thermodynamically favored addition product, FH_2N-HF. If reaction of the second F atom is stimulated by photolysis of the intermediate species $[H_2N^{\bullet}-HF\cdots F^{\bullet}]$, then the main reaction is H-atom abstraction. The yield of this product increases with increasing photon energy (decreasing wavelength).

e. Reaction $F + NH_2^{\bullet} \rightarrow NH + HF$. As shown above, the thermal reaction $F + NH_2^{\bullet}$ gives only the addition product, NH_2F. The energy diagram in Figure 5 indicates that this is the most stable product. It was shown previously by several authors that the gas-phase reaction of $F + NH_2^{\bullet}$ gives rise to highly vibrationally excited HF molecules (with population inversion).[16−18] The highly excited HF products were interpreted as being formed by a direct abstraction reaction, without the participation of a long-lived NH_2F intermediate.

In our experiment, the $[H_2N^{\bullet}-HF\cdots F^{\bullet}]$ radical pairs can decay by addition of F to $NH_2^{\bullet}$ (with a spectator HF molecule in the cage), or they can react by abstraction to form NH and a second HF molecule. The addition channel is observed exclusively for the thermal reaction; this is the expected result, because the ground electronic states of $F + NH_2^{\bullet}$ correlate adiabatically with NH_2F. In contrast, the photoinduced reaction occurs preferentially by abstraction. Gas-phase $NH_2^{\bullet}$ has a relatively long-lived $^2A_1$ excited state that is energetically accessible to the photolysis laser in our experiment. Reaction of this state with a F atom correlates to electronically excited states of the intermediate, but it is not clear why this should favor abstraction over addition as the principal product channel. We simply note that the gas-phase studies provide evidence that efficient channels do exist for direct abstraction reactions to occur in the absence of the matrix cage (which dissipates energy as needed to stabilize the NH_2F product).

4. Conclusions

Our analysis leads to the following conclusions about photochemical reactions of binary complexes NH_3-F_2 isolated in solid argon:

1. The main primary product of NH_3-F_2 photolysis is $[H_2N^{\bullet}-HF\cdots F^{\bullet}]$ radical pairs, which are stable at temperatures $T < 19$ K. In contrast to the usual case in which both F atoms generated by photolysis of a binary complex $M-F_2$ react with the molecule of the second reactant M, our observation of radical pair formation in this system is unique. We know of no other case in which cage escape of the partner F atom has been observed.

2. Thermal recombination of $[H_2N^{\bullet}-HF\cdots F^{\bullet}]$ radical pairs occurs at $T > 19$ K and leads exclusively to formation of FH_2N-HF. This $F + NH_2^{\bullet}$ recombination channel in solid argon is exactly the opposite of that in the gas phase, where the formation of NH and HF was observed earlier and direct abstraction of the H atom was suggested.

3. Electronic and vibrational excitation of $NH_2^{\bullet}$ in $[H_2N^{\bullet}-HF\cdots F^{\bullet}]$ radical pairs induces the return of the F atom and its reactions. The dominant product of these reactions is the NH−HF−HF complex. The relative yield of this product increases with increasing energy of photoexcitation and is close to unity at $\lambda < 355$ nm.

4. Deuterium and ^{15}N isotopic substitution results allowed the definitive assignment of infrared bands of the NH−HF−HF molecular complex, which was identified for the first time.

Acknowledgment. This paper is dedicated to Jack Beauchamp on the occasion of his 60th birthday. Financial support from the U.S. National Science Foundation (Grant CHE-9970032) and the Russian Foundation for Basic Research (Grant 01-03-33171) is gratefully acknowledged.

References and Notes

(1) Jacox, M. E. *Rev. Chem. Intermed.* **1985**, *6*, 77.
(2) Misochko, E. Ya.; Akimov, A. V.; Goldschleger, I. U.; Boldyrev A. I.; Wight, C. A. *J. Am. Chem. Soc.* **1999**, *121*, 405.
(3) Misochko, E. Ya.; Goldschleger, I. U.; Akimov, A. V.; Wight, C. A. *Low Temp. Phys.* **2000**, *26*, 727.
(4) Kunntu, H.; Feld, J.; Alimi, R.; Becker, A.; Apkarian, V. A. *J. Chem. Phys.* **1990**, *92*, 4856.
(5) Misochko, E. Ya.; Akimov, A. V.; Wight, C. A. *Chem. Phys. Lett.* **1997**, *274*, 23.
(6) Misochko, E. Ya.; Akimov, A. V.; Wight, C. A. *Chem. Phys. Lett.* **1998**, *293*, 547.
(7) Johnson, G. L.; Andrews L. *J. Am. Chem. Soc.* **1980**, *102*, 5736.
(8) Hunt, R. D.; Andrews, L. *J. Chem. Phys.* **1985**, *82*, 4442.
(9) Hunt, R. D.; Andrews, L. *Inorg. Chem.* **1987**, *26*, 3051.
(10) Andrews, L.; Lascola, R. *J. Am. Chem. Soc.* **1987**, *109*, 6243.
(11) Goldschleger, A. U.; Akimov, A. V.; Misochko, E. Ya.; Wight, C. A. *J. Mol. Spectrosc.* **2001**, *205*, 269.
(12) Abouaf-Margulin, L.; Jacox, M. E.; Milligan, D. E. *J. Mol. Spectrosc.* **1977**, *67*, 34.
(13) Misochko, E. Ya.; Benderskii, A. V.; Goldschleger, A. U.; Akimov, A. V.; Benderskii, V. A.; Wight, C. A. *J. Chem. Phys.* **1997**, *106*, 3146.
(14) *CRC Handbook of Chemistry and Physics*, 77th ed.; CRC Press: Boca Raton, FL, 1996−1997.
(15) Frisch, M. J.; Trucks, G. W.; Schlegel, H. B.; Scuseria, G. E.; Robb, M. A.; Cheeseman, J. R.; Zakrzewski, V. G.; Montgomery, J. A., Jr.; Stratmann, R. E.; Burant, J. C.; Dapprich, S.; Millam, J. M.; Daniels, A. D.; Kudin, K. N.; Strain, M. C.; Farkas, O.; Tomasi, J.; Barone, V.; Cossi, M.; Cammi, R.; Mennucci, B.; Pomelli, C.; Adamo, C.; Clifford, S.; Ochterski, J.; Petersson, G. A.; Ayala, P. Y.; Cui, Q.; Morokuma, K.; Malick, D. K.; Rabuck, A. D.; Raghavachari, K.; Foresman, J. B.; Cioslowski, J.; Ortiz, J. V.; Baboul, A. G.; Stefanov, B. B.; Liu, G.; Liashenko, A.; Piskorz, P.; Komaromi, I.; Gomperts, R.; Martin, R. L.; Fox, D. J.; Keith, T.; Al-Laham, M. A.; Peng, C. Y.; Nanayakkara, A.; Challacombe, M.; Gill, P. M. W.; Johnson, B. G.; Chen, W.; Wong, M. W.; Andres, J. L.; Gonzalez, C.; Head-Gordon, M.; Replogle, E. S.; Pople, J. A. *Gaussian 98*, revision A.9; Gaussian, Inc.: Pittsburgh, PA, 1998.
(16) Donaldson, D. J.; Sloan, J. J.; Goddard, J. D. *J. Chem. Phys.* **1985**, *82*, 4524.
(17) Wategaonkar, S.; Sester, D. W. *J. Chem. Phys.* **1987**, *86*, 4477.
(18) Goddard, J. D.; Donaldson, D. J.; Sloan, J. J. *Chem. Phys.* **1987**, *114*, 321.